GSA Data Repository 2018386 https://doi.org/10.1130/G45294.1

Direct Mesoproterozoic connection of Congo and Kalahari cratons in proto-Africa: Strange attractors across supercontinental cycles

Johanna Salminen[1], Richard Hanson[2], David A.D. Evans[3], Zheng Gong[3], Tierney Larson[3], Olivia Walker[3], Ashley Gumsley[4,5], Ulf Söderlund[4,6], and Richard Ernst[7,8]

[1]Department of Geosciences and Geography, University of Helsinki, 00014 University of Helsinki, Finland

[2]Department of Geological Sciences, Texas Christian University, Fort Worth, TX 76129, USA

[3]Department of Geology & Geophysics, Yale University, New Haven, Connecticut 06520, USA

[4]Department of Geology, Lund University, Lund223 62, Sweden

[5]Institute of Geophysics, Polish Academy of Sciences, Warsaw, 01-452, Poland

[6]Department of Geosciences, Swedish Museum of Natural History, Stockholm 11418, Sweden

[7]Department of Earth Sciences, Carleton University, Ottawa K1S 5B6, Canada

[8]Faculty of Geology and Geography, Tomsk State University, Tomsk 634050, Russia

S1. METHODS

S1.1 Geochronological methods

Baddeleyite is a common accessory phase in mafic intrusions and a proven U-Pb geochronometer. Therefore, the separation of baddeleyite was attempted on several mafic dolerite dike samples that were the least altered due to metamorphism, and were sufficiently coarse-grained. This separation

procedure was done at the Department of Geology, Lund University. The water-based separation technique of Söderlund and Johannsson (2002) was employed from cut and crushed rock, and was successful in yielding sufficient baddeleyite from samples W1518, S1601G and S1608G. These samples were studied for U-Pb geochronology, employing the same techniques as described by Gumsley et al. (2015) using isotope dilution thermal ionization mass spectrometry (ID-TIMS).

After handpicking, three fractions of the best-quality baddeleyites grains from each of the three samples were assembled. One to five grains per fraction were transferred to Teflon capsules in ethanol. The fractions were then rinsed repeatedly in ultrapure 7 M HNO_3 and H_2O to improve the Pb blank during measurement. For dissolution, an ultrapure HF:HNO_3 (10:1) solution was added to the individual Teflon capsules with a ^{205}Pb-$^{233-236}$U tracer solution. The capsules were placed for 3 days in an oven running at 190°C. After dissolution, the capsules were cooled and dried on a hot plate at 100°C. Ultrapure 6 M HCl together with 0.25 M H_3PO_4 was added to each capsule, and once again, the capsules were placed on a hot plate to dry down. The remaining droplet containing the sample fractions was dissolved in 2 uL silica gel before being loaded onto outgassed Re filaments.

The U and Pb isotopic compositions were measured at the Department of Geosciences in the Swedish Museum of Natural History using a Thermo Scientific - Finnigan TRITON mass spectrometer. The Pb isotope compositions of the samples were measured in dynamic (peak jumping) mode using a secondary electron multiplier at temperatures between 1210°C to 1240°C. Pb isotopes (^{204}Pb ^{205}Pb, ^{206}Pb and ^{207}Pb) were measured for between 80 and 120 cycles. U isotopes (^{233}U, ^{236}U and ^{238}U) were measured for between 40 and 120 cycles at temperatures between 1310°C and 1360°C, also in dynamic mode. The procedural blank in the isotope laboratory at the Swedish Museum of Natural History was determined to be 0.05 pg for U and 0.5 pg for Pb. Mass fractionation for Pb was determined by replicate analyses of the common and radiogenic NIST standard reference materials SRM 981 and SRM 983. The determination of U fractionation was obtained directly from the measured ^{233}U/^{236}U isotopic ratio. The Stacey and Kramers (1975)

modelled common Pb evolution curve was used to estimate the initial Pb compositions at the age of the sample. The decay constants used were 1.55125×10^{-11} (^{238}U) and 9.8485×10^{-10} (^{235}U), with the isotopic composition of U being $^{238}U/^{235}U = 137.88$ (Jaffey et al., 1971; Steiger & Jäger, 1977).

The uncertainty in age includes ± 0.04 in Pb fractionation and ± 50% in Pb and U blank concentration. Uncertainties in Pb blank composition are 2.0% for $^{206}Pb/^{204}Pb$ and 0.2% for $^{207}Pb/^{204}Pb$. The final treated analytical results were calculated and plotted using the Microsoft Excel Macro, Isoplot (Ludwig, 2003), excluding decay constant errors.

S1.2 Paleomagnetic methods

For paleomagnetic studies, we sampled 35 sites representing 34 separate cooling units (33 dikes and one sill) in the southern part of the Congo craton in Angola and in Namibia (Table DR2). Sampled dikes trend from N-S to NNW-SSE. The dikes show vertical to subvertical dips at sites where the contacts between dikes and host rocks are visible. Sill S1608 intrudes quartzite (bedding 33° toward 025°); an apophysis from the sill penetrates the overlying quartzite, confirming an intrusive relationship. Samples were mainly taken with the portable water-cooled gasoline field drill. Block samples were taken from one of the dikes (site S1646). Six to twelve oriented 2.5-cm-diameter core samples were collected from each cooling unit. Baked host and unbaked host rock at eight sites were sampled (at site S1610 only block samples were taken) for baked contact tests (Everitt and Clegg, 1962). Six to 25 samples were collected from each baked contact test site. Cored samples were oriented using solar and magnetic compasses, whereas block samples were oriented using magnetic orienting. We screened possible effects of lightning strikes on outcrops with a magnetic compass. Due to limited sizes of outcrops, minor deflections were unavoidable at a few sites. Cored samples were cut into several specimens with a non-magnetic dual-blade saw at Yale University. Specimens were split into two parts, which were measured in the magnetically shielded room of the paleomagnetic laboratory at the Department of Geology and Geophysics at Yale

University, USA, and in the Solid Earth Geophysics Laboratory at the University of Helsinki, Finland. At Yale University after measurement of the natural remanent magnetization (NRM), the samples were cycled through the Verwey transition at ~ 120° K (Verwey, 1939) by immersing them in liquid nitrogen in order to reduce the viscous component carried by larger magnetite grains (Schmidt, 1993). The specimens were then thermally demagnetized using a nitrogen-atmosphere ASC Scientific model TD-48SC furnace. At the University of Helsinki part of the specimens underwent stepwise demagnetization using the in-line static 3-axis alternating field (AF) system paired to a 2G cryogenic magnetometer, and part were thermally demagnetized using an argon-atmosphere ASC Scientific model TD-48SC furnace. Demagnetization was continued until the magnetic intensity of the specimens dropped below system noise level or until the measured directions became erratic and unstable. Both the thermal and AF (for most of the samples) methods were effective and results from both laboratories are comparable.

Principal-component analysis (Kirschvink, 1980; Jones, 2002) was used to isolate the characteristic remanent magnetization (ChRM) for specimens displaying near-linear demagnetization trajectories. The best-fit line was used if defined by at least five consecutive demagnetization steps that trended toward the origin. The maximum angle of deviation (MAD) was less than 10° for most of the accepted specimens. At sites S1601, S1602, S1604, and S1605 MAD as high as 25° was accepted for some of the specimens if the obtained direction was in line with the directions of the specimens with lower MAD from the same cooling unit. The mean directions were calculated using Fisher statistics (Fisher, 1953) to compute a site mean, giving unit weight to each sample (in cases of two specimens per sample each specimen was assigned 0.5 weight). The site mean was accepted for further calculation if it was obtained from four or more separate samples. We used the constant cutoff angle of 45° commonly used to exclude transitional virtual geomagnetic poles (VGPs) (e.g., Johnson et al., 2008). The maximum deviation of VGPs from the mean paleopole was 41°.

S2. RESULTS

S2.1 Geochronological results

The extracted baddeleyite grains from the samples were between 20 μm and 50 μm in length and are medium brown in color. In sample W1518, a total of three baddeleyite fractions were analyzed (Bd1–3; Table DR1), with each fraction being composed of between two and three grains. Regression comprising the three fractions yields upper and lower intercepts of 1109 ± 10 Ma and 447 ± 270 Ma, respectively (with a MSWD < 0.1; Fig. 3). Concordance varies between □96% and □99%, with the most concordant baddeleyite fraction having a $^{207}Pb/^{206}Pb$ date of 1101 ± 3 Ma (2σ). We interpret the upper intercept age of 1109 ± 10 Ma to to date crystallization of this intrusion. A subordinate fraction of baddeleyite in all these samples have frosty surfaces, indicative for secondary zircon formed during a later event of alteration or metamorphism. We thus attribute the lower intercept of 447 ± 270 Ma to a younger Cambrian (possibly Pan-African) event during which baddeleyite was partly converted to zircon in the presence of silica.

The three fractions of sample S1601G plot moderately discordant (2-3 %), and have scattered $^{207}Pb/^{206}Pb$ dates between 1115 Ma and 1097 Ma which precludes meaningful linear regression and a conclusive age interpretation for this sample. The weighted $^{207}Pb/^{206}Pb$ mean is 1104 ± 4 Ma (2σ) but is associated with a high MSWD value of 7.1. If discordance of individual fractions was the result of a Pan-African thermal event combined with younger (recent?) diffusional Pb-loss, as depicted in Figure 3 by the two dotted reference lines from 1110 Ma to 550 Ma and from 1110 Ma to 0 Ma, that could explain the scattered analyses. We admit the ambiguous result of this sample and therefore only an approximate age of ~1104 Ma (the weighted mean of $^{207}Pb/^{206}Pb$ dates) can be assigned to this sample.

Three fractions (Bd1–3), with between 1 and 3 baddeleyite grains in each fraction, were analyzed for sample S1608G (Table DR1). These fractions produced $^{207}Pb/^{206}Pb$ dates between 1129 Ma and 1097 Ma. We favor the weighted mean of $^{207}Pb/^{206}Pb$ dates of the two near-

concordant fractions Bd-1 and Bd-2, i.e. 1127 ± 8 Ma, as the most reliable age estimate for this sample (Fig. 3).

S2.2 Paleomagnetic results

Most dike sites exhibited one or two components of remanent magnetization (Fig. DR1). Based on thermomagnetic analyses and unblocking temperatures (~ 500- 580°C) the ChRM is typically carried by (titano)magnetite. The ChRM of sill S1608 is carried by both magnetite and hematite (Fig. DR1) and due to age difference from the dikes this is excluded from the mean. Twenty-three of the accepted sites show consistent ChRM with shallow to intermediate, mainly upward directions, generally with SW declination, and two of the accepted sites show ChRM with shallow downward directions with NE declination (Table DR2; Fig. DR2). The mean directions of these two polarity groups pass the reversal test of McFadden and McElhinny (1990), but the classification level is indeterminate due to low number of sites showing the NE declination (obtained angle between the directions: 18.2° and critical angle: 25.2°; Table DR2). Two of the most westerly Angolan sites (S1629 and S12EN) and one site from Namibia (JS1508) show NW-down and WSW-down directions, which are interpreted to date from regional low-grade metamorphism of Ediacaran-Cambrian age (possibly related to the adjacent Kaoko orogen). Site S12EM, which shows scattered ChRM directions, is one of the most westerly Angolan sites and samples were moderately weathered. Site S1654 also shows scattered ChRM directions: low- to moderate-temperature and low-coercivity remanent magnetization components for these samples were scattered and not coherent enough to produce clustered means for mean calculations.

Host rocks at eight sites were sampled for baked contact tests (Figs. DR3 and DR4). Reliability of the new HE dikes pole is supported by a baked-contact test on site L14E07 in Namibia (Fig. DR3). The ~100-m wide dike yields intermediate SW-upward ChRM typical for the HE swarm. Several baked foliated mafic gneiss samples 1.3–50 m from the dike margin show

ChRM directions similar to the dike. Samples between 35 m and 100 m from the dike margin commonly show steep upward NW directions. For a second test, sill site S1608 yields a shallow SW-downward ChRM, and baked quartzite in contact with the top of the sill shows a similar shallow SW subhorizontal magnetization direction; subhorizontal purple mudstones ~100m higher in the sedimentary succession show a similar direction, but it is not certain whether this indicates pervasive remagnetization of the sedimentary strata, or whether they are only slightly older than the sill. Attempted baked contact tests for sites S1602, S1655, L14E05, and L14E06 were inconclusive mainly due to scattered ChRM directions in the host rock. The ChRM for dike D1604 is horizontal with SW declinations, but baked host-rock samples show both horizontal East (unblocking below 580°C) and horizontal West (unblocking below 350°C) directions.

TABLES

TABLE S1. ID-TIMS BADDELEYITE ISOTOPIC DATA FROM THE DIKES W1518 AND S1601 AND FROM THE SILL S1608

Analysis number (number of grains)	U/Th	Pbc/ Pbtot*	$^{206}Pb/^{204}Pb$ raw†	$^{207}Pb/^{235}U$ [corr]§	± 2σ % err.	$^{206}Pb/^{238}U$ [corr]§	± 2σ % err.	Rho	$^{207}Pb/^{235}U$ [age, Ma]	± 2σ abs. err.	$^{206}Pb/^{238}U$ [age, Ma]	± 2σ abs. err.	$^{207}Pb/^{206}Pb$ [age, Ma]	± 2σ abs. err.	Concordance
S1608G - 1127 ± 8 Ma (weighted mean $^{207}Pb/^{206}Pb$)															
Bd-1 (1 grain)	13.8	0.702	48.3	1.9996	2.2498	0.1876	1.2925	0.61	1115.4	15.2	1108.4	13.2	1129.0	35.6	98.2
Bd-2 (2 grains)	10.4	0.245	223.8	1.9828	0.7743	0.1862	0.6494	0.82	1109.7	5.2	1100.8	6.6	1127.1	8.9	97.7
Bd-3 (3 grains)	0.6	0.093	466.3	1.8682	0.6123	0.1781	0.5315	0.85	1069.9	4.0	1056.5	5.2	1097.3	6.5	96.3
S1601G - ca. 1104 Ma															
Bd-1 (3 grains)	7.9	0.139	443.2	1.9392	0.9692	0.1832	0.8979	0.90	1094.7	6.5	1084.5	9.0	1115.1	8.6	97.3
Bd-2 (3 grains)	0.6	0.067	682.3	1.9026	0.9353	0.1813	0.8718	0.90	1082.0	6.2	1074.3	8.6	1097.6	8.1	97.9
Bd-3 (5 grains)	9.3	0.064	1005.3	1.9110	0.6205	0.1822	0.5732	0.90	1084.9	4.1	1079.1	5.7	1096.6	5.4	98.4
W1518 - 1109 ± 10 Ma (upper intercept)															
Bd-1 (2 grains)	48.0	0.123	375.4	1.8058	1.5939	0.1736	1.5295	0.92	1047.6	10.4	1031.7	14.6	1080.7	12.5	95.5
Bd-2 (2 grains)	47.1	0.044	982.7	1.9311	0.3398	0.1837	0.3022	0.87	1091.9	2.3	1087.2	3.0	1101.4	3.4	98.7
Bd-3 (3 grains)	35.0	0.164	261.2	1.9055	0.7891	0.1815	0.6589	0.82	1083.0	5.3	1075.3	6.5	1098.7	9.0	97.9

Note: Sample S1608G is from the sill S1608; sample S1601G is from the dike S1601, sample W1518 is from the dike W1518

* Pbc = common Pb; Pbtot = total Pb (radiogenic + blank + initial).

† Measured ratio, corrected for fractionation and spike.

§ Isotopic ratios corrected for fractionation (0.1% per amu for Pb), spike contribution, blank (0.5 pg Pb and 0.05 pg U), and initial common Pb. Initial common Pb corrected with isotopic compositions from the model of Stacey and Kramers (1975) at the age of the sample.

166

167

168 TABLE DR2. PALEOMAGNETIC DATA FOR EACH SITE IN HUILA-EPEMBE MAFIC INTRUSIONS

Site	Age (Ma)	SLat (°S)	SLon (°E)	N/n	B	D (°)	I (°)	k	a95 (°)	PLat (°N)	PLon (°E)
S1608[*†]	1127±8[§]	16.71205	13.14839	4/7	0	237.3	17.4	24.9	18.8	-34.2	283.0
										K=31.5	A95=16.6
S1601[#]	ca. 1104[§]	17.33856	13.92666	10/13	1	024.4	20.7	18.0	11.7	52.7	056.2
S1605[#]		17.32328	13.89552	6/8	1	039.1	08.7	07.2	26.7	45.3	078.3
S1602[†]		17.33205	13.87869	6/7	1	212.5	-15.1	11.8	20.4	-49.4	250.3
S1604		17.33114	13.88415	6/8	1	231.5	-34.5	19.0	15.8	-27.7	250.0
S1606		17.29864	13.92193	6/8	1	204.1	-37.6	11.2	20.9	-43.2	223.1
S1607[*]		16.99194	13.72447	5/9	0	306.2	10.2	06.8	31.7	-	-
S1629[*]		15.68298	12.26259	8/12	0	252.2	46.3	07.0	22.6	-	-
S1637		15.52762	13.31250	6/9	1	242.1	-09.3	17.3	16.6	-25.4	270.0
S1638, S12EK		15.51881	13.34103	8/12	1	232.7	20.3	12.4	16.4	-38.9	285.2
S1642	1110 ± 3[**]	15.26252	13.55929	6/11	1	234.3	-09.4	16.4	17.0	-32.9	267.2
S1646		15.05847	13.22374	8/13	1	214.1	-22.2	67.5	06.8	-46.9	246.8
S1647		14.87991	13.13260	9/9	1	206.0	-05.8	10.4	16.7	-58.5	250.7
S1650		14.72857	13.34138	8/12	1	213.6	-05.7	24.1	11.5	-52.5	258.7
S1651[*]		14.71335	13.33191	7/8	0	152.9	19.7	13.7	16.9	-	-
S1654[*§§]		14.67431	13.35023		0	-	-			-	-
S1655[†]		14.67432	13.35103	7/7	1	221.3	-15.6	57.4	08.0	-43.2	257.0
S1659		14.71807	13.39359	8/13	1	266.4	-13.1	26.5	11.0	-01.7	275.9
S12EI[†]		15.56163	13.26660	5/6	1	218.6	-18.1	29.8	14.2	-44.2	252.8
S12EJ main[*]		15.52745	13.30506	7/7	0	166.5	05.2	63.2	07.7	-	-
S12EJ satellite		15.52745	13.30506	6/6	1	266.9	-15.9	161.2	05.3	-00.7	274.6
S12EM[*§§]		15.88349	12.23204		0	-	-			-	-
S12EN[*]		15.88396	12.25305	5/5	0	347.0	61.3	103.5	07.6	-	-
JS15A07		17.22023	13.64281	10/10	1	263.8	-06.0	28.5	09.2	-05.0	278.8
JS15A08[*]		17.21996	13.64217	5/5	0	260.4	73.3	11.2	23.9	-	-
L14E05+D1607[†]		17.55524	13.57151	12/12	1	246.2	-34.7	46.4	06.4	-15.6	256.7
L14E06[†]		17.55206	13.58556	6/6	1	271.7	-34.4	46.7	09.9	07.2	265.6
L14E07[††]		17.55484	13.58333	8/8	1	221.8	-36.9	84.5	06.1	-33.9	242.5
W1516		17.52081	13.53650	10/10	1	216.3	-40.8	17.3	11.9	-35.1	233.9
W1517		17.52904	13.53037	8/8	1	216.6	02.1	28.0	10.7	-50.5	262.9
W1518	1109 ± 10[§]	17.52966	13.52843	7/7	1	232.0	-52.8	52.4	8.4	-18.0	237.1
D1603		17.54996	13.57063	10/10	1	240.3	-32.3	51.0	6.8	-21.2	255.8
D1604[†]		17.60256	13.65184	5/5	1	230.9	-09.5	33.8	13.3	-35.0	264.4
D1606		17.57945	13.66880	10/10	1	184.8	-26.0	6.6	20.3	-55.2	201.9
MEAN				**191/228**	**25**	**228.3**	**-20.7**	**10.0**	**9.6**	**-34.7**	**256.5**
										K=12.1	**A95= 8.7**
Means for reversal test[***]											
MEAN NE (polarity inverted)				12/15	2	212.1	-14.9			-49.7	248.3
MEAN SW				179/213	23	229.9	-21.1	9.6	10.3	-33.1	257.1
Obtained angles of reversal test										γ=18.2	γ_c=25.2

169 Note: SLat, SLon are the site latitude and longitude. N (n) is the number of samples (specimens) used to calculate the
170 paleomagnetic declination (D) and inclination (I); a95 and k are the 95% confidence envelope and the concentration
171 parameter for the paleomagnetic direction. B is the number of sites used for a between-site mean direction, where 1(0)
172 indicates sites included (excluded) for calculation of the mean direction. PLat and PLon are the latitude and longitude of
173 the virtual geomagnetic pole (VGP). A95 and K are the 95% confidence envelope and the concentration parameter for
174 VGP distribution. γ (γ_c) is obtained (critical) angle between the mean directions of different polarities (McFadden and
175 McElhinny, 1990).
176 *Site excluded from the calculation of the mean direction.
177 †Site for attempted baked contact test.
178 §Age from this study.
179 #Polarity of the ChRM direction has been reversed for mean pole calculation
180 **Age from Ernst et al. (2013).

181 ††Site for positive baked contact test.
182 §§Significantly scattered within-site directions.
183 ***Reversal test of McFadden and McElhinny (1990) using software of Koymans et al. (2016)
184

185 TABLE DR3. PALEOMAGNETIC POLES USED FOR THE ~1.1 Ga RECONSTRUCTION

Pole	Plat (°N)	Plon (°E)	A95	Reference	Age (Ma)	Age references
Congo						
Huila-Epembe	-34.7	256.5	8.7	This work	1109 ± 10; 1110 ± 3: ca. 1104	This work; Ernst et al., 2013
Kalahari						
Umkondo mean	-64.0	222.1	2.6	Swanson-Hysell et al., 2015	1108.6 ± 1.2; 1112.0 ± 0.5	Hanson et al., 2004 (range of ages)
Laurentia						
Seagull intrusions	42.0	233.4	7.1	Borradaile and Middleton, 2006	1112.8 ± 1.4	Heaman et al., 2007
Coldwell Complex (R) centers A,B,C	46.8	203.1	4.2	Kulakov et al., 2014	1108 ± 1	Heaman and Machado, 1992
Mamainse Point volcanics–Lower R1	47.5	226.7	8.0	Swanson-Hysell et al., 2009	n/a	
Powder Mill Group (R) (Siemens Creek Formation)	45.8	214.0	9.2	Palmer and Halls, 1986	1107.3 ± 1.6	Davis and Green, 1997
Osler Volcanics–R	43.1	194.5	5.9	Halls, 1974	1107.4 +5/-4; 1105 ± 2	Davis and Green, 1997

186 Note: Plat – pole latitude; Plong – pole longitude; A95 – 95% confidence circle of the pole

187

188

189

190 FIGURES

191

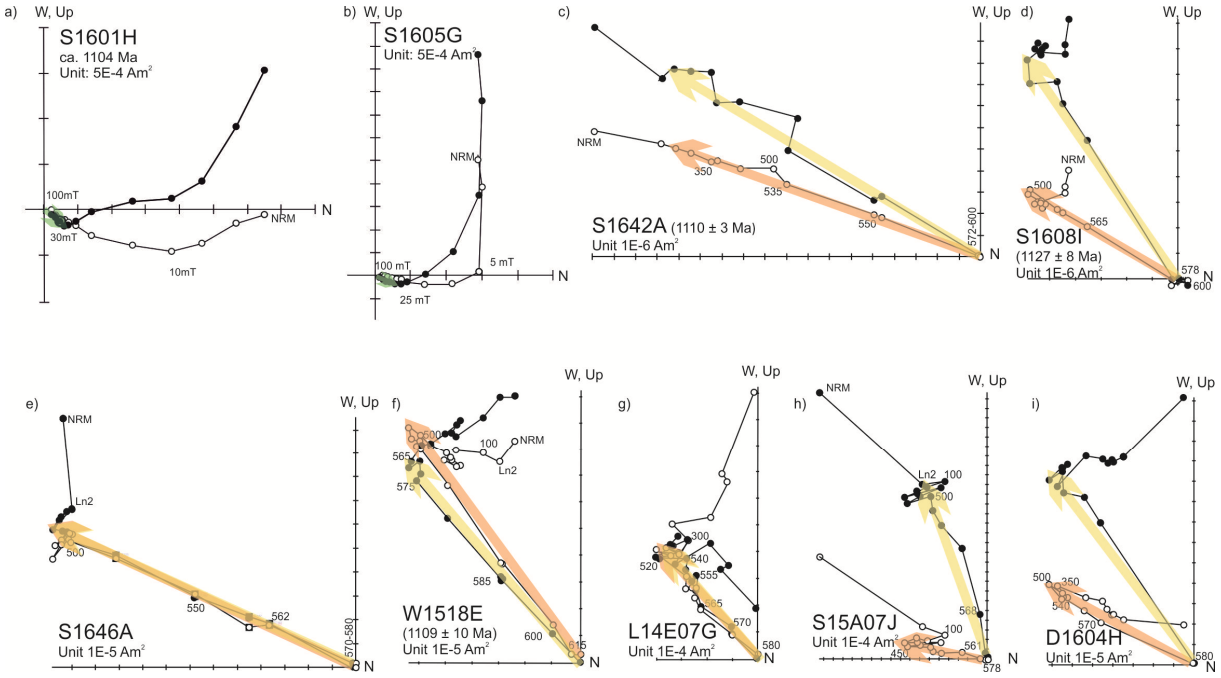

192

193 **Figure DR1**. Typical orthogonal vector plots of demagnetization (vertical/horizontal projections
194 shown by open/filled symbols) from mafic intrusions in Angola and Namibia for samples from
195 eight dikes and for one sample from a sill (S1608I). Numbers (with mT) indicate thermal (AF)
196 demagnetization step.

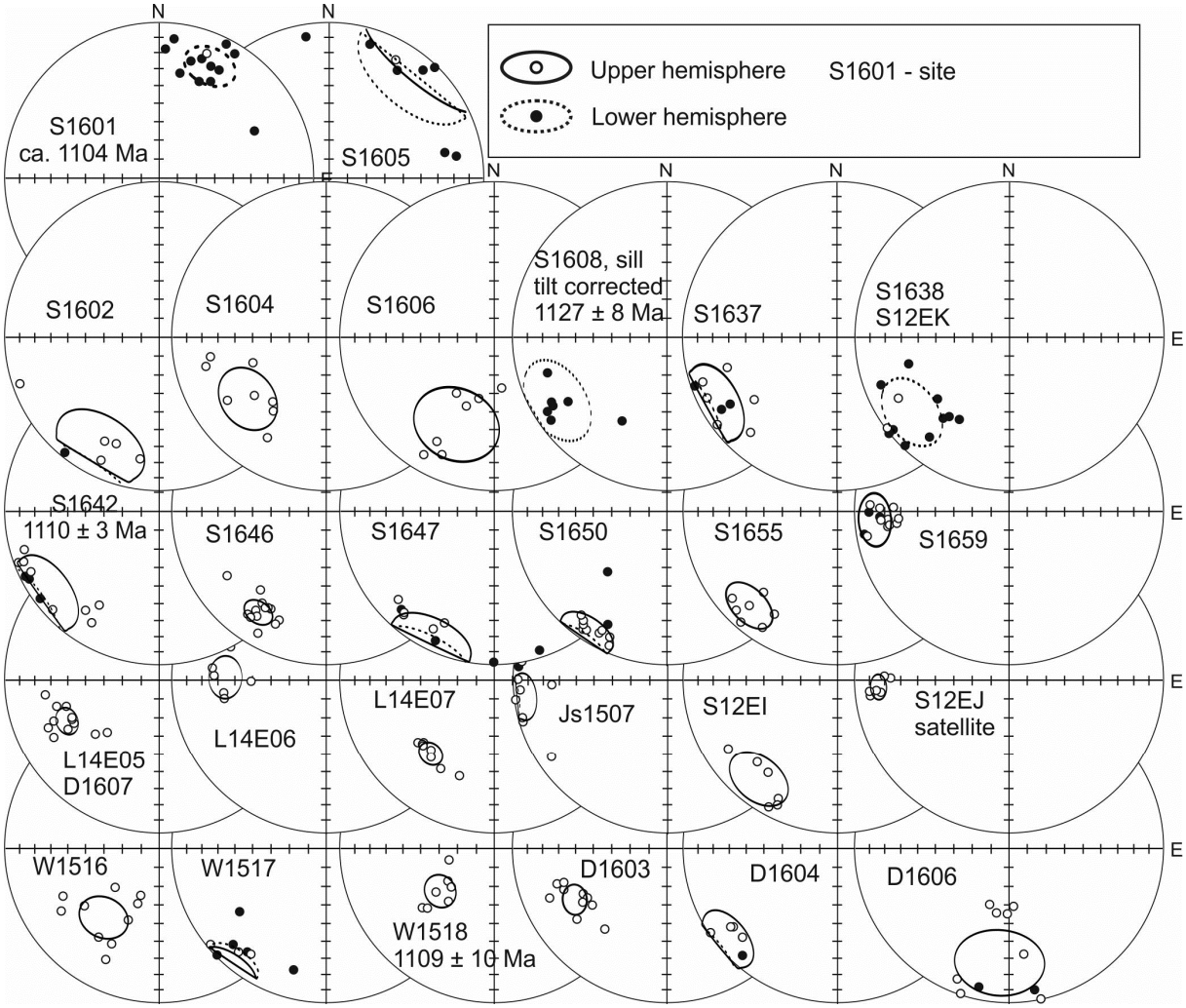

Figure DR2. Site-mean paleomagnetic remanence directions for twenty-five HE dikes and one sill in Angola and Namibia (Table DR2). Sill site S1608 was excluded from the mean due to age difference with other included sites. Tilt correction for the sill S1608 was done according to the bedding of the overlying, intruded quartzite (strike 295°, dip 33°NE) (see section 1.2.). Stereoplots show the paleomagnetic directions with the 95% confidence circle for each site. Open/closed symbol indicate upper/lower hemisphere. U-Pb ages given for three sites are from Ernst et al. (2013) and this work.

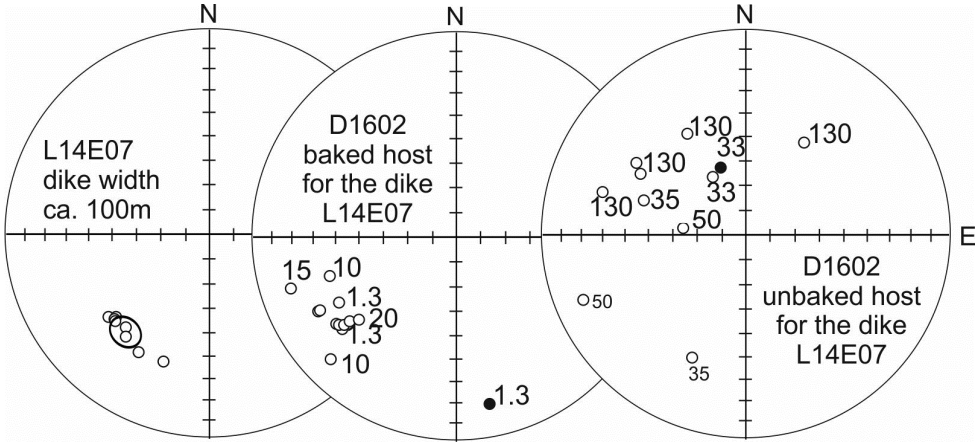

207

208 **Figure DR3**. Positive baked contact test for the Epembe dike L14E07; numbered points indicate
209 host-rock distances in meters from the dike contact. Open/closed symbols indicate upper/lower
210 hemisphere.

211

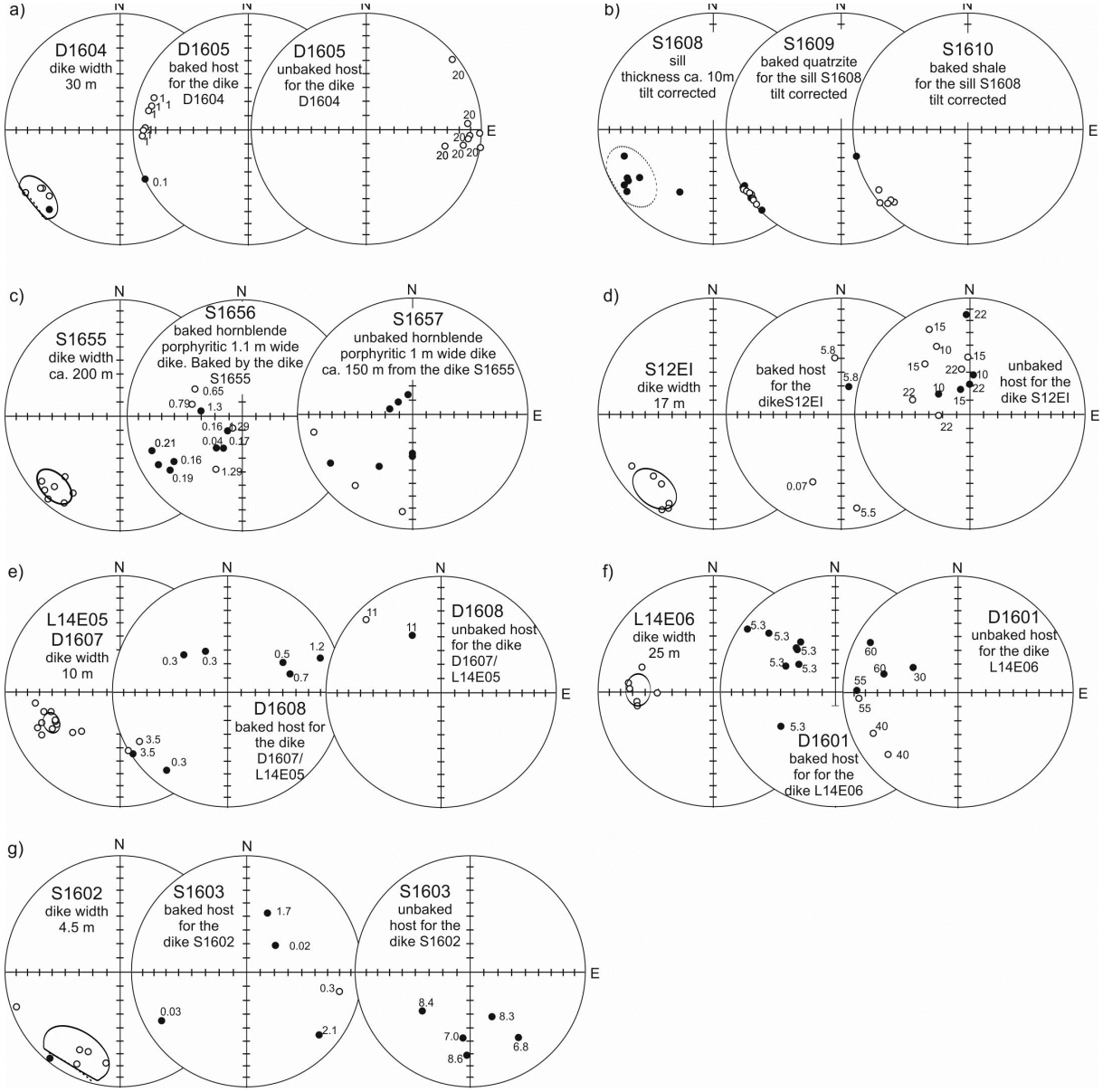

Figure DR4. Paleomagnetic results of attempted baked contact tests for six of the HE dike sites and for one sill in Namibia and Angola. Tilt correction for the sill S1608 was done according to the bedding of the overlying, intruded quartzite (strike 295°, dip 33°NE). Bedding of the purple shale 100m stratigraphically higher than the quartzite is subhorizontal (strike 175°, dip 07°W). Open/closed symbols indicate upper/lower hemisphere. Numbers for baked and unbaked host rock samples denote the distance from the dike margin in meters.

REFERENCES CITED

Borradaile, G.J., Middleton, R.S., 2006, Proterozoic paleomagnetism in the Nipigon Embayment of northern Ontario: Pillar Lake Lava, Waweig Troctolite and Gunflint Formation tuffs: Precambrian Research, v. 144, 69-91.

Davis, D., and Green, J. C., 1997, Geochronology of the North American Midcontinent rift in western Lake Superior and implications for its geodynamic evolution: Canadian Journal of Earth Sciences, v. 34, p. 476–488.Ernst, R.E., Pereira, E., Hamilton, M.A., Pisarevsky, S.A., Rodriques, J., Tassinari, C.C.G., Teixeira, W., and Van-Dunem, V., 2013, Mesoproterozoic intraplate magmatic 'barcode' record of the Angola portion of the Congo Craton: Newly dated magmatic events at 1505 and 1110 Ma and implications for Nuna (Columbia) supercontinent reconstructions: Precambrian Research, v. 230, p. 103–118, https://doi.org/10.1016/j.precamres.2013.01.010.

Everitt, C.W.F., and Clegg, J.A., 1962, A field test of paleomagnetic stability: Geophysical Journal of London, v. 6, p. 312-319.

Fisher, R.A., 1953, Dispersion on a sphere: Proceedings of the Royal Society, ser. A, v. 217, p. 295–305.

Gumsley, A., Olsson, J., Söderlund, U., de Kock, M., Hofmann, A., Klausen, M., 2015, Precise U-Pb baddeleyite age dating of the Usushwana Complex, southern Africa: Implications for the Mesoarchaean magmatic and sedimentological evolution of the Pongola Supergroup, Kaapvaal Craton: Precambrian Research v. 267, p. 174–185.

Halls, H. C., 1974, A paleomagnetic reversal in the Osler Volcanic Group, Northern Lake Superior: Canadian Journal of Earth Sciences, v. 11, p. 1200–1207.

Hanson, R.E., Crowley, J.L., Bowring, S.A., Ramazani, J., Gose, W.U., Dalziel, I.W.D., Pancake, J.A., Seidel, E.K., Blenkinsop, T.G., Mukwakwami, J., 2004, Coeval large-scale magmatism in the Kalahari and Laurentian cratons during Rodinia assembly: Science v. 304, p. 1126–1129.

Heaman, L. M., and N. Machado, 1992, Timing and origin of Midcontinent rift alkaline magmatism, North America: Evidence from the Coldwell Complex: Contributions to Mineralogy and Petrology, v. 110, p. 289–303.

Heaman, L.M., Easton, R.M., Hart, T.R., MacDonald, C.A., Hollings, P., Smyk, M., 2007, Further refinement to the timing of Mesoproterozoic magmatism, Lake Nipigon region, Ontario: Canadian Journal of Earth Science, v. 44, 1055-1086.

Jaffey, A,H,, Flynn, K.F., Glendenin, L.E., Bentley, W.C., and Essling, A.M., 1971, Precision measurement of half-lives and specific activities of U^{235} and U^{238}: Physical Review C 4 p. 1889–1906.

Johnson, C.L., Constable, C., Tauxe, L., Barendregt, R., Brown, L., Coe, R., Layer, P., Mejia, V., Opdike, N., Singer, B., Staudigel, H., and Stone, D., 2008, Recent investigations of the 0–5 Ma geomagnetic field recorded by lava flows: Geochemistry Geophysics Geosystems, v. 9, , Q04032, doi: 10.1029/2007GC001696.

Jones, C.H., 2002, User-driven integrated software lives: "PaleoMag" Paleomagnetics analysis on the Macintosh: Computers & Geosciences, v. 28, p. 1145–1151.

Kirschvink, J L., 1980, The least squares line and plane and the analysis of paleomagnetic data: Geophysical Journal of the Royal Astronomical Society, v. 62, p. 699–718.

Koymans, M.R., Langereis, C.G., Pastor-Galan, D., and van Hinsbergen, D.J.J., 2016. Paleomagnetism.org: An online multi-platform open source environment for paleomagnetic data analysis: Computers and Geosciences, v. 93, p. 127–137.

Kulakov, E.V., Smirnov, A.V., and Diehl, J.F., 2014, Paleomagnetism of the ~1.1 Ga Coldwell Complex (Ontario, Canada): Implications for Proterozoic geomagnetic field morphology and plate velocities: Journal of Geophysical Research Solid Earth, v. 119, p. 8633–8654.

Ludwig, K.R., 2003, User's Manual for Isoplot 3.00—A Geochronological Toolkit for Microsoft Excel (Berkeley Geochronology Center, Berkeley, CA), Special Publication 4.

McFadden, P.L., and McElhinny, M.W., 1990. Classification of the reversal test in paleomagnetism: Geophysical Journal International, v. 103, p. 725–729.

Palmer, H. C., and Halls, H. C., 1986, Paleomagnetism of the Powder Mill Group, Michigan and Wisconsin: A reassessment of the Logan Loop: Journal of Geophysical Research, v. 91, p. 11,571–11,580.

Schmidt, P.W., 1993, Paleomagnetic cleaning strategies: Physics of the Earth and Planetary Interiors, v. 76, p. 169–178.

Söderlund, U., and Johansson L., 2002, A simple way to extract baddeleyite (ZrO_2): *Geochemistry* Geophysics Geosystems **3**, http://dx.doi.org/10.1029/2001GC000212.

Stacey, J.S., and Kramers, J.D., 1975, Approximation of terrestrial lead isotope evolution by a two-stage model: Earth and Planetary Science Letters v. **26**, p. 207–221.

Steiger, R.H., and Jäger, E., 1977, Subcommission on geochronology: Convention on the use of decay constants in geo- and cosmochronology: Earth and Planetary Science Letters v. 36, p. 359–362.

Swanson-Hysell, N.L., Maloof, A.C., Weiss, B.P., and Evans, D.A.D., 2009, No asymmetry in geomagnetic reversals recorded by 1.1-billion-year-old Keweenawan basalts: Nature Geoscience, v. 2, p. 713–717.

Swanson-Hysell, N.L., Kilian, T.M., and Hanson, R.E., 2015, A new grand mean palaeomagnetic pole for the 1.11 Ga Umkondo large igneous province with implications for palaeogeography and the geomagnetic field: Geophysical Journal International, v. 203, p. 2237–2247.

Verwey, E.J.W., 1939, Electronic conduction of magnetite (Fe_3O_4) and its transition point at low-temperature: Nature, v. 44, p. 327–328.